ACS APPLIED BIO MATERIALS

Article

Discovery of Specific Nonpeptide Probe for Chymotrypsin via Molecular Docking-based Virtual Screening and the Application

Hao Xiong, Rong-Rong Li, Shi-Yu Liu, Feng-Xu Wu, Wen-Chao Yang, and Guang-Fu Yang

ACS Appl. Bio Mater., **Just Accepted Manuscript** • DOI: 10.1021/acsabm.8b00072 • Publication Date (Web): 06 Jul 2018

ACS Publications

is published by the American Chemical Society. 1155 Sixteenth Street N.W., Washington, DC 20036

Discovery of Specific Nonpeptide Probe for Chymotrypsin *via* Molecular Docking-based Virtual Screening and the Application

Hao Xiong [a, †], *Rong-Rong Li* [a, †], *Shi-Yu Liu* [a], *Feng-Xu Wu* [a], *Wen-Chao Yang* [a*], *Guang-Fu Yang* [a,b *]

[a]Key Laboratory of Pesticide & Chemical Biology, Ministry of Education, and Chemical Biology Center, College of Chemistry, Central China Normal University, Wuhan 430079, P.R. China;

[b]Collaborative Innovation Center of Chemical Science and Engineering, Tianjin 30071, P.R. China.

[†]The first two authors contribute equally to this work.

*Wen-Chao Yang, e-mail: tomyang@mail.ccnu.edu.cn; Tel: +86-27-67867706; Fax: +86-27-67867141; Guang-Fu Yang, e-mail: gfyang@mail.ccnu.edu.cn; Tel: +86-27-67867800; Fax: +86-27-67867141.

ABSTRACT. Chymotrypsin is a proteolytic enzyme associated with numerous biological processes. Moreover, it has been reported to be significantly involved in pancreatic diseases. Thus, its rapid and sensitive detection is of great significance for early diagnosis and related drug discovery. Herein, a new strategy of molecular docking-based virtual screening (MDVS) was developed for the identification of a new nonpeptide-based biosensor targeting chymotrypsin. The newly discovered probe, numbered probe **20**, exhibits about 45-fold specificity toward chymotrypsin over the similar enzyme trypsin, and produces about 250-fold higher increase of fluorescence intensity under the catalysis of chymotrypsin. Furthermore, the probe successfully allowed the characterization of the kinetics of chymotrypsin inhibitors. More importantly, the endogenous chymotrypsin in *zebrafish* was visualized by nonpeptide probe for the first time, demonstrating the potential of the probe **20** for future application in the mechanistic study or clinic diagnosis for pancreatic diseases. Accordingly, the MDVS strategy could be generally applied in the identification of specific fluorescent probe for a particular enzyme.

INTRODUCTION

Chymotrypsin (E.C. 3.4.21.1), a serine-type hydrolase, plays an important role in the digestive systems of many organisms. This proteolytic enzyme has a higher hydrolytic efficiency than its similar enzyme trypsin, and it is usually used as medicine for treating rhinitis, sinusitis, pharyngitis, lung abscess and other otorhinolaryngologic diseases.[1] Recent studies have showed that chymotrypsin was associated with tissue repair[2-4] and pathogenesis of multiple diseases.[5-9] Thus, the development of bioanalytical methods for chymotrypsin sensing is of great significance to the clinical diagnostics and therapy of associated disorders.

Fluorescent probe-based biosensors have recently received a lot of attention due to their fast, convenient and economical features.[10] The subjects of discovering those chemosensors vary from small reactive molecules (biothiols, ions, amino acids, etc.)[11-15] to biomacromolecules (enzymes, protein receptors, etc.)[16-19] in biological systems, and even some probes can be retrofitted to detect physical parameters such as pH[20], pressure[21] and temperature.[22] We have mainly focused on discovering fluorescent probes for particular enzymes in the past few years and have identified several chemical probes for certain serine hydrolases.[23-26] Previously, we developed a fluorogenic and chromogenic assay for monitoring the activity of chymotrypsin with the first reported nonpeptide-based fluorescent probe (termed as **Probe 2**), with a randomly screening strategy that introduced some simple recognition groups to the same fluorophore.[25] This probe could be hydrolyzed by chymotrypsin for which it displays 5-fold higher binding affinity with obvious "OFF-ON" signal. Interestingly, this probe has lower costs than the traditional peptide-based probe **AMC-FPAA-Suc** used in chymotrypsin sensing. However, it only causes about 25-fold increase in fluorescence intensity (FI) with a limit of detection (LOD) of around 50 ng/mL. Moreover, although the that probe can discriminate chymotrypsin from the similar digestive

enzyme trypsin, the corresponding selectivity ratio is only about 14.5-fold, which impedes its application for specific chymotrypsin imaging *in vivo*.

Herein, we report the discovery of a new small-molecule fluorescence-quenched probe with a completely new recognition group for selective chymotrypsin sensing *via* a novel strategy of molecular docking-based virtual screening (MDVS, Fig. 1a). In general, MDVS is composed of the following three steps. Firstly, we built a virtual compound library (Table S1) in which we designed various aromatic rings as the recognition group by mimicking the non-polar aromatic side-chain of the native peptide substrate, and the methoxyfluorescein was preserved as the fluorophore. Secondly, we screened the interaction of those compounds with chymotrypsin (PDB code: 2P8O) by molecular docking. Thirdly, we calculated the interaction energies of the top poses for each chymotrypsin-compound complex. Thereafter, compounds **7, 20 and 33** bearing thiophene ring attached with different length of methylene chains (n = 0, 1, 2) were selected as the best hits for organic synthesis and kinetic characterization (Fig. 1b). Finally, a new small molecule (**20**) was identified as a specific chymotrypsin probe. Due to its thorough fluorescence quenching by the thiophene ring, the probe **20** demonstrated excellent features for the detection of chymotrypsin in aqueous solution with ~250-fold higher enhancement in FI and ~8.4 ng/mL of the LOD. Most interestingly, that probe shows more than 45-fold selectivity ratio for chymotrypsin over trypsin and therefore enabled the successful imaging of the endogenous chymotrypsin in *zebrafishes* for the first time. These findings demonstrate its good capability for imaging and visualizing chymotrypsin in complicated biological samples.

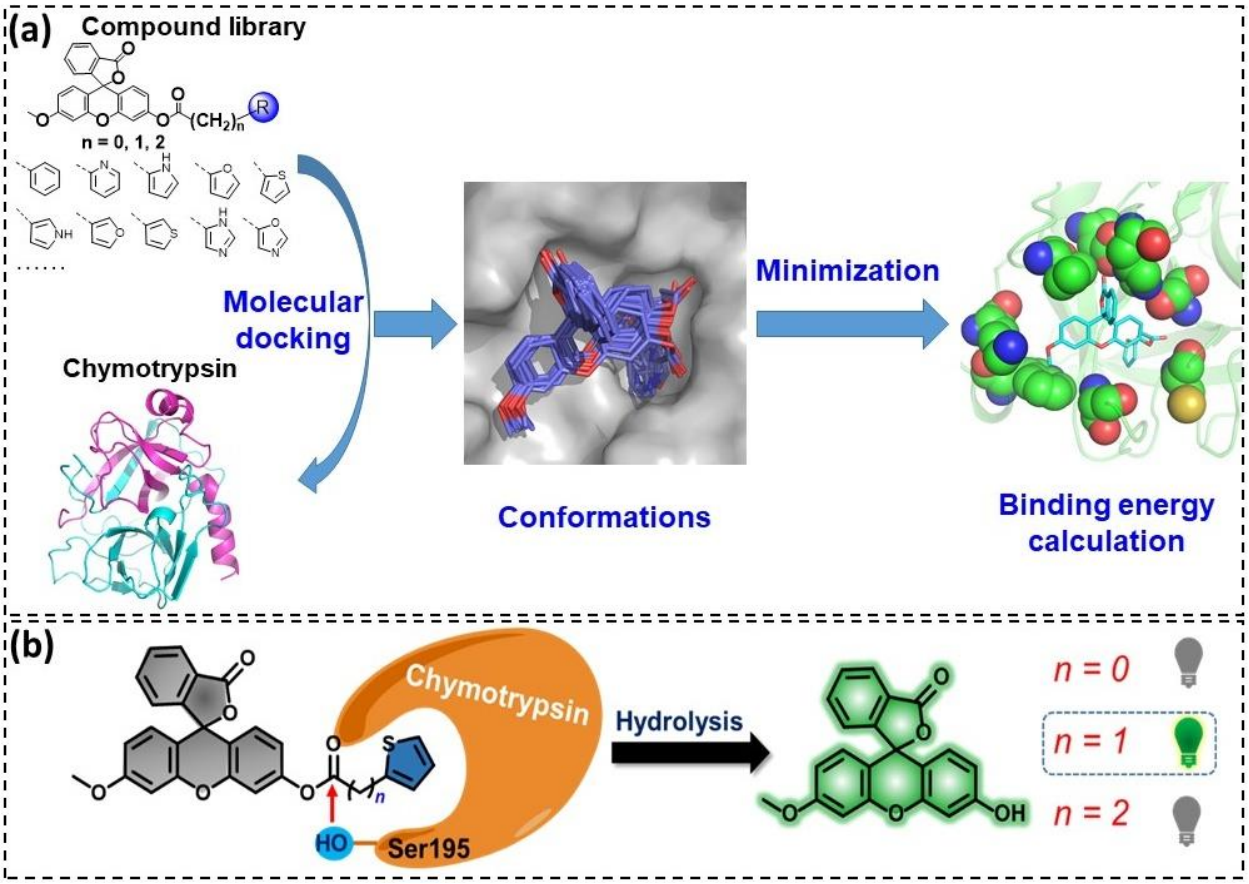

Fig. 1 (a) The workflow of MDVS. (b) The chemical mechanism of designed probes for sensing chymotrypsin.

EXPERIMENTAL SECTION

Reagents. Unless specific statements, all original reagents used in synthesis were commercially available and bought from regular manufacturers; the silica gel (200-300 mesh) used in the column chromatography was provided by Qingdao Haiyang Chemical Co., Ltd of Shandong province in China and enzymes used in this work were purchased from Sigma-Aldrich. Besides, the solvent was purified and dried through traditional methods before experiments.

Instruments.

In organic-synthesis parts, NMR experiments (^{1}H NMR for all compounds and ^{13}C NMR only for target probes) were performed on the Varian Mercury Plus 600 MHz (or 400 MHz) spectraphotometer, and the samples were dissolved with DMSO-d_6 or $CDCl_3$ and taking tetramethylsilane (TMS) as 0 ppm of the chemical shift (δ). High-Resolution Mass Spectrometry (HRMS) and High-Performance Liquid Chromatography (HPLC) experiments were operated on SYNAPT G2 HDMS (MALDI; MA, USA) and Agilent 1200 (ZORBAX SB-C18 Colum), respectively. Besides, the NMR data and relevant graphs in the characterizations for all the probes were dealt with MestReNova 9.0.1 and OriginLab 2018, respectively.

In probe characterization parts, The Ultraviolet-Visible (UV-Vis) spectroscopy and emission spectra of fluorescence were both obtained with the microplate reader (M5, Molecular Devices), while the inhibitory studies of the probes were recorded by black 96-well microplates on the instrument.

Organic Synthesis.

Synthesis of the MeF-OH. The synthetic procedures of both the intermediates (**M1** and **MeF-OH)** were obtained according to the previous reports[23-25], which were indicated in **Scheme 1**.

Scheme 1. Synthetic peocedures of the fluorophore.

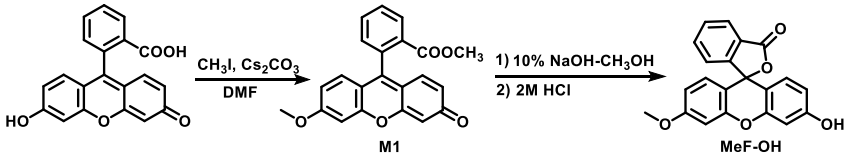

Synthesis of the target probe 07 (Scheme 2). In the solution of anhydrous dichloromethane (DCM) was added the prearranged fluorophore **MeF-OH** (346 mg, 1.0 mmol). Then the Et_3N

(151.5 mg, 1.5 mmol) was added slowly into the above solution. Later, the 2-thiophenecarbonyl chloride (293.2 mg, 2.0 mmol) was added dropwise under 0 ^{o}C. Then the reaction mixture was extracted with water (2×) and saturated salt water (1×) after stirring for 2 hours at room temperature. In the following, the organic phase was dried with anhydrous sodium sulfate and subsequently evaporated under the reduced pressure. The target probe **7** (233 mg, 51.1%) was eventually purified through silica gel chromatography (Petroleum ether : Acetone = 20:1 to 10:1) . ^{1}H NMR (400 MHz, DMSO-d_6) δ 8.12 (d, J = 5.0 Hz, 1H), 8.09-8.02 (m, 2H), 7.80 (dt, J = 27.3, 7.4 Hz, 2H), 7.44 (d, J = 2.2 Hz, 1H), 7.40-7.30 (m, 2H), 7.09 (dd, J = 8.7, 2.3 Hz, 1H), 6.98 (d, J = 2.3 Hz, 1H), 6.91 (d, J = 8.7 Hz, 1H), 6.80-6.70 (m, 2H), 3.84 (s, 3H). ^{13}C NMR (150 MHz, $CDCl_3$) δ 169.42, 161.59, 160.13, 153.15, 152.38, 152.03, 151.89, 135.26, 135.21, 134.12, 132.40, 129.99, 129.22, 129.12, 128.27, 126.61, 125.22, 124.13, 117.58, 117.04, 112.11, 111.03, 110.53, 101.00, 82.58, 77.22. HRMS calcd for $[M + H]^+$457.4755; found: 457.4749.

Synthesis of the target probe 20 (Scheme 2). With the same procedures, 2-thiopheneacetyl chloride (321.1 mg, 2.0 mmol) was added to the solution and the product **20** (243 mg, 51.7%) was obtained. ^{1}H NMR (600 MHz, DMSO-d_6) δ 8.04 (d, J = 7.6 Hz, 1H), 7.78 (dt, J = 37.1, 7.5 Hz, 2H), 7.47 (d, J = 5.0 Hz, 1H), 7.34 (d, J = 7.6 Hz, 1H), 7.27 (d, J = 2.1 Hz, 1H), 7.09 (d, J = 3.0 Hz, 1H), 7.02 (d, J = 5.0 Hz, 1H), 6.99-6.92 (m, 4H), 6.88 (d, J = 8.7 Hz, 1H), 6.79-6.69 (m, 2H), 4.26 (s, 2H), 3.83 (s, 3H). ^{13}C NMR (150 MHz, $CDCl_3$) δ 169.40, 168.53, 161.51, 153.03, 152.26, 151.90, 151.85, 135.26, 133.95, 129.98, 129.19, 129.10, 127.39, 127.10, 126.49, 125.57, 125.19, 124.05, 117.30, 116.98, 112.06, 110.86, 110.25, 100.88, 82.49, 55.68, 35.58. HRMS calcd for $[M + H]^+$471.5025; found: 471.5033.

Synthesis of the target probe 33 (Scheme 2). The prearranged fluorophore **MeF-OH** (346 mg, 1.0 mmol), 3-(2-thienyl) propionic acid (312.4 mg, 2.0 mmol) and *3*-

(ethyliminomethylideneamino)-N, N-dimethylpropan-1-amine, hydrochloride (EDCI, 384 mg, 2.0 mmol) and *4-dimethylaminopyridine* (DMAP, 60 mg) were subsequently added into a round-bottomed flask containing DCM (25 mL). After stirring the reaction system for about 3 hours at room temperature, the reaction was almost completed by TLC monitoring. Then the probe **33** (117 mg, 24.2%) was obtained with the same post-treatment process. ^{1}H NMR (600 MHz, DMSO-d_6) δ 8.10 (d, J = 7.4 Hz, 1H), 7.91 – 7.81 (m, 3H), 7.73 (d, J = 8.4 Hz, 1H), 7.32 – 7.27 (m, 1H), 7.00 – 6.83 (m, 5H), 6.75 – 6.64 (m, 1H), 3.86 (s, 3H), 3.00 (t, J = 7.4 Hz, 3H), 2.56 (t, J = 7.4 Hz, 3H).^{13}C NMR (100 MHz, $CDCl_3$) δ 178.17, 170.60, 164.79, 151.85, 151.01, 142.73, 142.50, 134.34, 133.71, 133.13, 131.59, 129.80, 129.06, 127.02, 125.05, 124.82, 123.86, 123.71, 122.99, 119.10, 115.45, 112.88, 105.20, 55.99, 36.27, 35.86, 25.13, 24.85. HRMS calcd for [M + H]$^{+}$485.5295; found: 485.5290.

Scheme 2. Synthetic route of the target probes **7**, **20** and **33**.

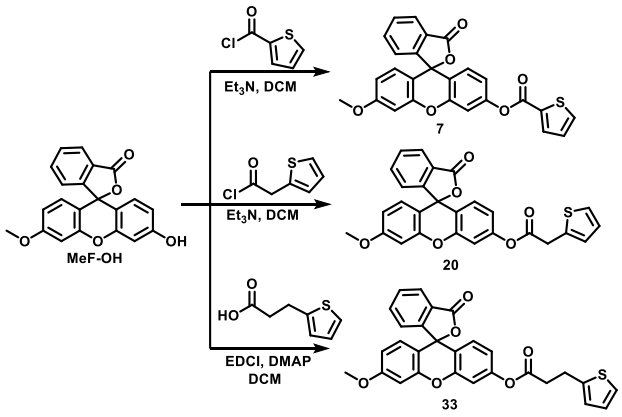

Computational Chemistry

Structures Preparation for Docking. Receptor structure (PDB ID: 2P8O)[27] was obtained from Protein Data Bank, probe molecules were constructed by Sybyl2.0 and optimized in tripos

force field. Autodock Tools 1.5.6 was applied to assign Gasteiger charges for the receptor. And it was also used as the utility to assign Gasteiger charges and rotatable bonds for small molecules.

Docking Experiments. Autodock 4.2.5 was used to perform the docking work[28]. The grid size was set to be 60 × 64 × 68 for all the simulated docking study. The grid was set at default value of 0.375 Å. The conformational search of the Autodock was accomplished by lamarkian genetic algorithm (LGA). The binding model analysis for all the probes was obtained from the best poses selected.

Fluorometric Assays

The assays were carried out by using the peptide (**AMC-FPAA-Suc**) and the newly synthesized probe with the procedures described in the previous report, respectively.[25]

Live Image with *Zebrafish*

Zebrafishes were preserved in E3 embryo media (0.15 mM KCl, 0.33 mM $MgSO_4$, 0.33 mM $CaCl_2$ and 5 mM NaCl, pH = 7.0 ± 1.0) for 3-5 days before used. After replacement into glass bottom dishes, *zebrafishes* were pretreated with 2 μM tacrine and 2 μM TPCK for 20 min before incubation with 10 μM probe **20** for 10 min, the fluorescence images were then acquired by inverted fluorescence microscopy (Olympus IX71, Japan) with a 4× objective lens.

RESULTS & DISCUSSIONS

The Identification of Potential Hits *via* MDVS.

The workflow of MDVS is shown in Fig. 1a. In the virtual probe library (see Table S1), we reserved the methoxyfluorescein, the fluorophore, and introduced various aromatic rings as the recognition group by mimicking the aromatic side-chain of the natural peptide substrate. More

specifically, those aromatic rings include benzene, pyridine, pyrrole, thiophene, furan, imidazole, thiazole and oxazole. They are linked with the ester group through the methylene chain at different length (-CH_2- unit) from 0 to 2, adjusting the conformation of the whole recognition group when binding into the chymotrypsin active site. After the computational screening by the molecular docking and the energy minimization for all the 39 compounds in the library, the compound **20** bearing the thiophene ring attached with one-carbon methylene was obtained as the best hit. For a clear comparison, the simulated binding modes for the three probes (**7**, **20** and **33**) with methylene chain of 0-2 carbon atoms are depicted in Fig. 2. According to the theory of *catalytic triad*[29-31], the closest distance of Ser195 to the ester bond of the probe most possibly indicates the easiest initiation of the nucleophilic attack. Apparently, it is found that probe **20** shows the nearest distance (3.4 Å) between its carbonyl group and the key residue Ser195 in the active site, whereas **7** or **33** exhibits much further distances (4.1 Å and 4.3 Å) for their carbonyl groups with the key residue Ser195, respectively. To understand the effect of the methylene chain against the flexibility of the recognition group, all three probes were selected for chemical synthesis and further evaluation.

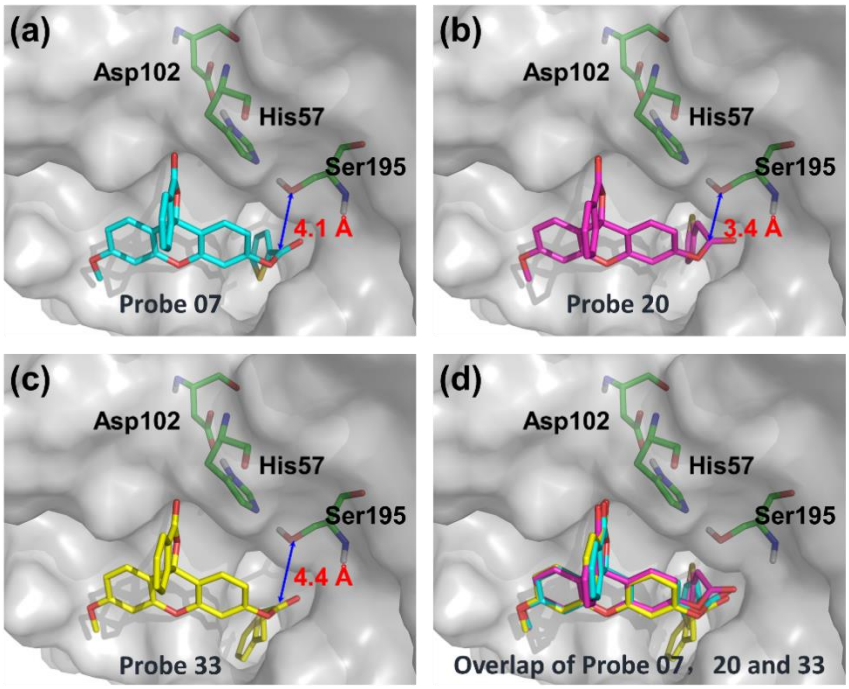

Fig. 2 The simulated binding models of probes **7** (a), **20** (b), **33** (c), and their superimposition (d) in the active site of chymotrypsin. The catalytic triad of His57, Asp102 and Ser195 are displayed in green sticks. The distance between the carbonyl group of the probes and Ser195 (key amino acid residue) is shown with blue arrow lines.

Chymotrypsin Detection and the Specificity of the Probes.

After the synthesis and characterization of the target probes (Fig. S1-S6), the optical properties were studied in HEPES buffer (100 mM, ≤ 0.5% DMSO, pH = 8.0) that only contains less than 0.5% dimethyl sulfoxide (DMSO). All of them display good water solubility and their fluorescence are quenched well (Fig. S7). As mentioned before, the best pH value for chymotrypsin is optimized from 7.8 to 8.0, and thus we chose pH 8.0 as the working pH. Basically, in the presence of chymotrypsin, enzymatic reaction cleaves the ester group of the

designed probes, then the fluorescein fluorophore becomes the open-ring form and the fluorescence can be tracked accordingly. Then we measured their response ability against chymotrypsin at aqueous solution. Obviously, probe **7** showed some response toward chymotrypsin but the specificity is very poor, while the probe **33** exhibited almost no hydrolysis upon the addition of chymotrypsin (Fig. 3a and Fig. 3c). On the contrary, the probe **20** displayed remarkable time-dependent FI increase under the catalysis of chymotrypsin (Fig. 3b). Intriguingly, probe **20** demonstrates the best response to chymotrypsin, while other tested hydrolases trigger no significant interference. Based on the measure of the relative reaction rate ($\Delta F/\Delta t$), it could be found that the selectivity of probe **20** is more than 45-fold for chymotrypsin over trypsin. In addition, the hydrolysis of probe **20** was examined under the interference of other small analytes, including metal ions (K^+, Mn^{2+}, Fe^{3+}, Co^{2+}, Na^+, Cu^{2+}) and amino acids (Glu, IIe, Cys, Asp, etc.). As expected, none of those small-molecule analytes caused significant interference against the sensing of chymotrypsin by probe **20**. Therefore, the following experiments were only emphasized on probe **20** in further experiments.

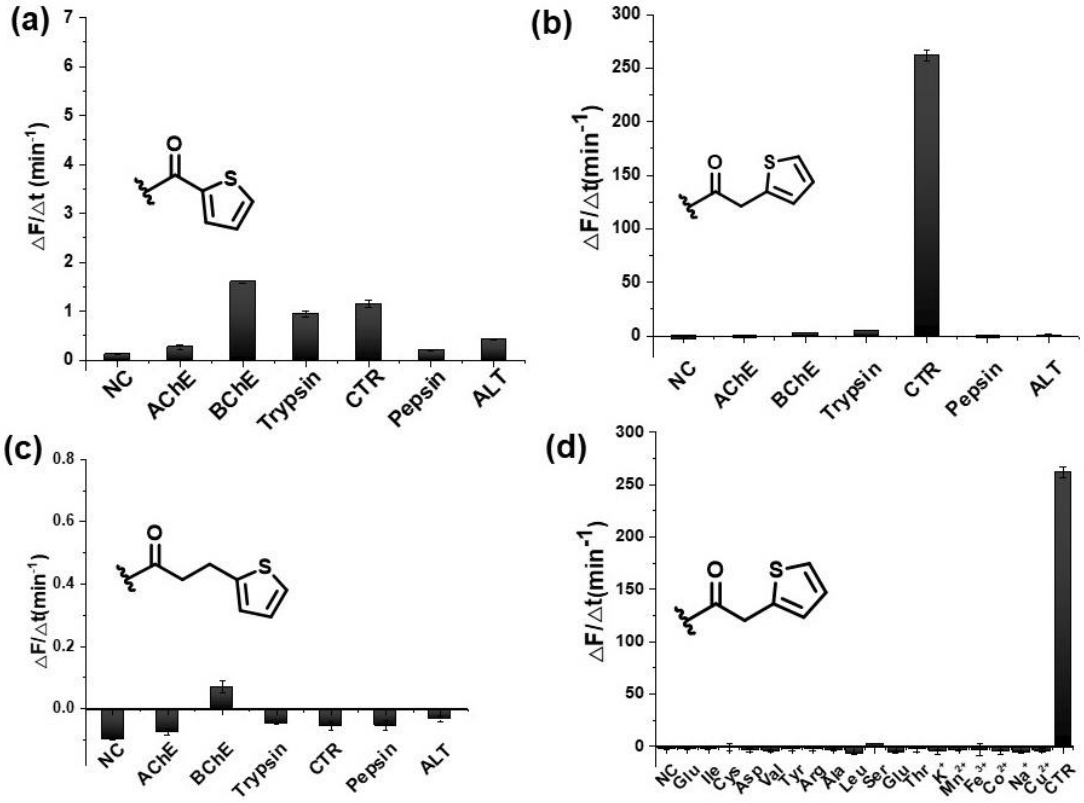

Fig. 3 Specificity profile of probes **7** (a), **20** (b) and **33** (c) (10 μM, respectively) towards common enzymes. The enzymes (20 μg/mL, individually) were kept in HEPES buffer (100 mM, ≤ 0.5% DMSO, pH = 8.0), at 30 ºC. NC refers to the rate of spontaneous hydrolysis. The meaning of abbreviations: AChE = acetylcholinesterase, CTR = chymotrypsin, ALT = alanine aminotransferase. (d) Specificity profile of probe **20** against the amino acids (1 mM, individually) and the metal ions (1 mM, individually).

Optical Characterizations of the Probe.

The time-dependent fluorescence spectrum (λ_{ex} = 455 nm) of the the probe **20** in HEPES buffer (100 mM, ≤ 0.5% DMSO, pH = 8.0) was investigated after the introduction of chymotrypsin. Notably, a remarkable increase in green fluorescence was observed time-dependently for the probe **20** when incubated with chymotrypsin, and the FI almost reached the

maximum after 40 minutes. The maximum FI at 515 nm reveals nearly 250-fold enhancement over the basal level (Fig. 4a). To further test the feasibility for the quantitative detection of chymotrypsin, the FI of probe **20** was investigated among different concentrations of chymotrypsin (0-20 μg/mL, in Fig. 4b). The graph showed that the augmentation of FI is dose-dependent with a linear correlation between the probe **20** and the concentration of chymotrypsin ranging from 0 to 4.0 μg/mL. By using *3σ/k* (calculation of LOD) method[32-33], the LOD for this probe was eventually determined to be ~8.40 ng/mL. These results show that **20** could offer a sensitive and robust fluorometric "OFF-ON" system for measuring the activity of chymotrypsin.

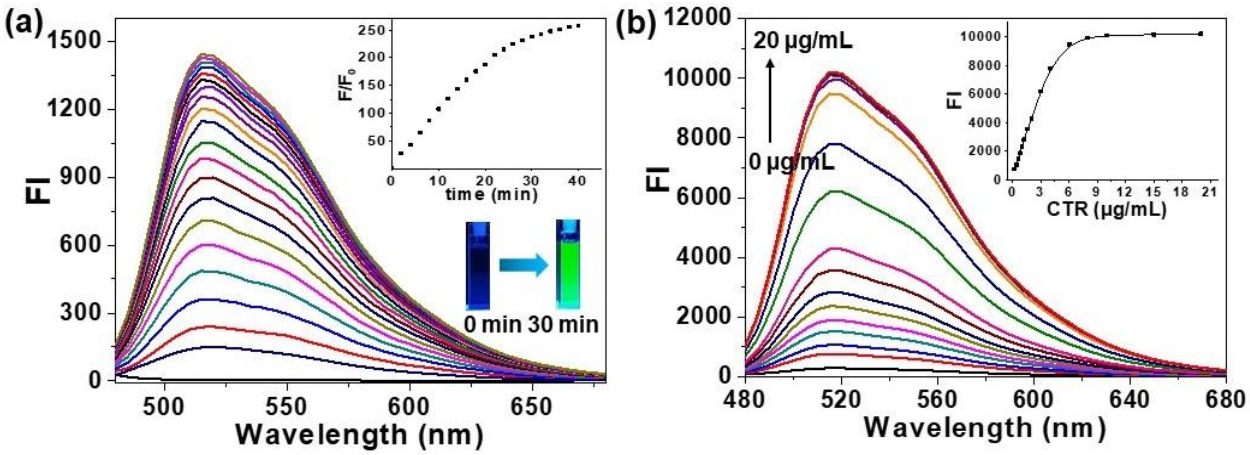

Fig. 4 Time-dependence (a) and concentration-dependent fluorescence spectra (b) of the probe **20** (10 μM) at the excitation of 455 nm. The experiments were performed in HEPES buffer (100 mM, ≤ 0.5% DMSO, pH = 8.0), at 30 ºC. The up inset in (a) describes the time-dependent FI enhancement at the maximum emission (λ_{em} = 515 nm) over the basal level and the down inset show the photos of the corresponding reaction mixtures before and after the incubation with chymotrypsin (0.02 U/mL) after 30 min at 30 °C. The inset in (b) provides the chymotrypsin concentration-dependent fluorescence increase at the maximum emission (λ_{em} = 515 nm).

Sensing Mechanism of the Probe.

To further validate the sensing mechanism, the HPLC experiment was used to analyze the solution of the probe **20** with or without the addition of chymotrypsin (Fig. 5). Specifically, the two individual groups dissolved with probe **20** were treated with (red curve) or without (black curve) chymotrypsin (20 μg/mL), while the similar solution of **MeF-OH** was also prepared under the same condition as the positive control. After the incubation for an hour , we could find that the peak of the probe **20** (t_R = 9.1 min) shrinked while the peak of the fluorophore (**MeF-OH**, t_R = 5.0 min) accordingly grew higher in the reaction system. The above observation indicates that the probe **20** was indeed hydrolyzed once the ester bond was broken up by chymotrypsin, generating the **MeF-OH** as the major product.

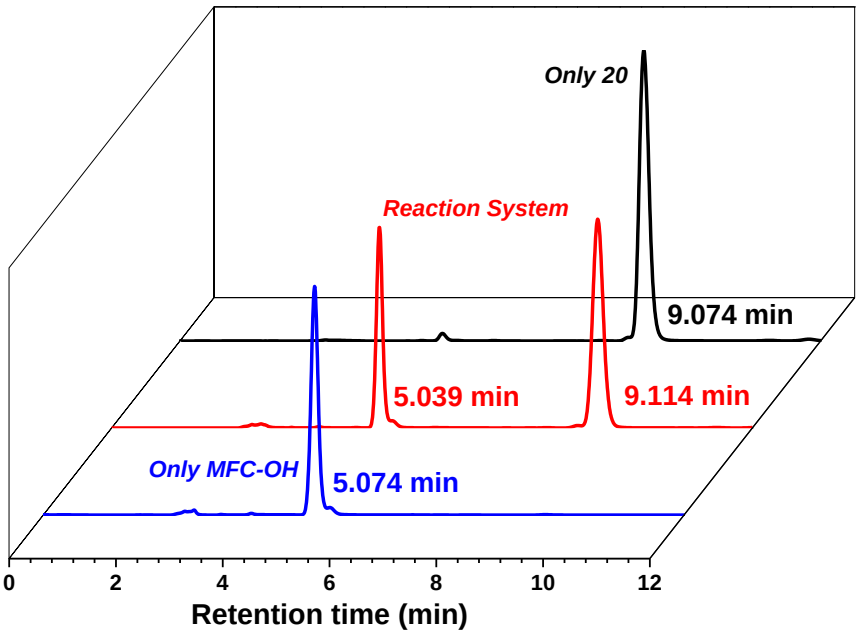

Fig. 5 HPLC spectrum of the probe **20** (20 μM) without (black curve) and with (red curve) the addition of chymotrypsin (20 μg/mL) incubated for 1 h in HEPES buffer (100 mM, ≤ 0.5% DMSO, pH = 8.0) at 30 °C. **MeF-OH** (the fluorophore, blue curve) was used as control.

Enzyme Kinetics and Inhibition

To highlight the effectiveness of probe **20** as substrate, the kinetics of chymotrypsin-catalysis of **20** was characterized with the widely used peptide substrate (**AMC-FPAA-Suc**) as reference. In general, the reaction rates for early stage of the chymotrypsin-catalyzed hydrolysis of each substrate were derived from the fluorescence response depending on the concentration of the probe 20 (0-20 μM) and **AMC-FPAA-Suc** (0-100 μM), respectively. As anticipated, the curves describing the kinetic changes of velocity depending on the increasing concentration of **20** and **AMC-FPAA-Suc** obey the Michaelis–Menten equation (Fig. 6). Subsequently, the Michaelis constant (K_m) for **20** and **AMC-FPAA-Suc** were determined to be 3.37 ± 0.41 μM and 58.84 ± 6.47 μM, respectively, implying that probe **20** shows a ~16-fold higher binding affinity towards chymotrypsin than **AMC-FPAA-Suc**. Although the catalytic constant (k_{cat}) of **20** (1.21 ± 0.41·min^{-1}) is much lower than that of **AMC-FPAA-Suc** (210 ± 15 min^{-1}), the overall catalytic efficiency of **20** (~0.33 $\mu M^{-1}\cdot min^{-1}$) is still comparable with that of **AMC-FPAA-Suc** (~3.62 $\mu M^{-1}\cdot min^{-1}$). In addition, the synthetic cost of **20** is less than 50 ¥/g before optimization, whereas the purchase price of **AMC-FPAA-Suc** from Wuhan Fine Peptide Co., Ltd. is over 500 ¥/mg. Thus, the cost of the probe **20** is about 10000-fold lower than that of **AMC-FPAA-Suc**. The above data suggests that probe **20** is a suitable substrate for the kinetic measurement of chymotrypsin.

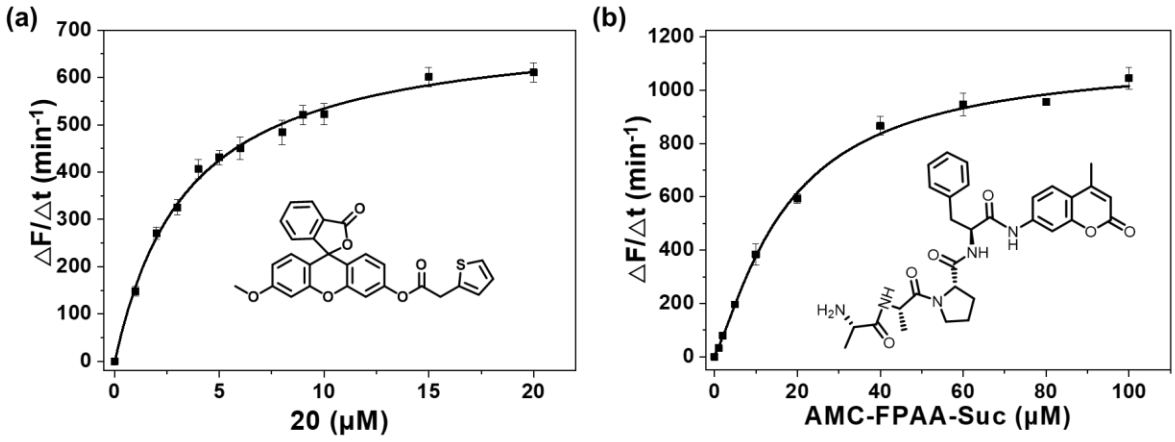

Fig. 6 Michaelis-Menten curve of the probe **20** (a) and **AMC-FPAA-Suc** (b) catalyzed by chymotrypsin (10 μg/mL for **20** and 0.02 μg/mL for peptide substrate, respectively) in HEPES buffer (100 mM, ≤ 0.5% DMSO, pH = 8.0, 30 °C) assessed using the fluorometric method.

To further investigate the ability of applying the probe **20** in chymotrypsin-targeted drug discovery, the inhibitor characterization was carried out with the probe **20**-based fluorometric assay in the presence of two well-known chymotrypsin inhibitors (phenylmethyl sulfonyl fluoride (PMSF) and chymostatin). Again, the **AMC-FPAA-Suc**-based fluorometric assay was used as reference for the characterization of the inhibitors. The plots describing the residual activity *vs* the concentration of inhibitors for the probe **20**-based assay are listed in Fig. 7, while the plots for peptide-based assay are indicated in Fig. S8. The resultant IC_{50} values derived from assay with **20** as substrate are 2.97 ± 0.074 μM for PMSF and 0.26 ± 0.02 μM for chymostatin, respectively, which are close to those obtained with **AMC-FPAA-Suc** as substrate (3.55 ± 0.17 μM for PMSF and 11.73 ± 0.95 nM for chymostatin). This inhibitory kinetic analysis provides another evidence that the probe **20** is a specific fluorescent probe targeting chymotrypsin.

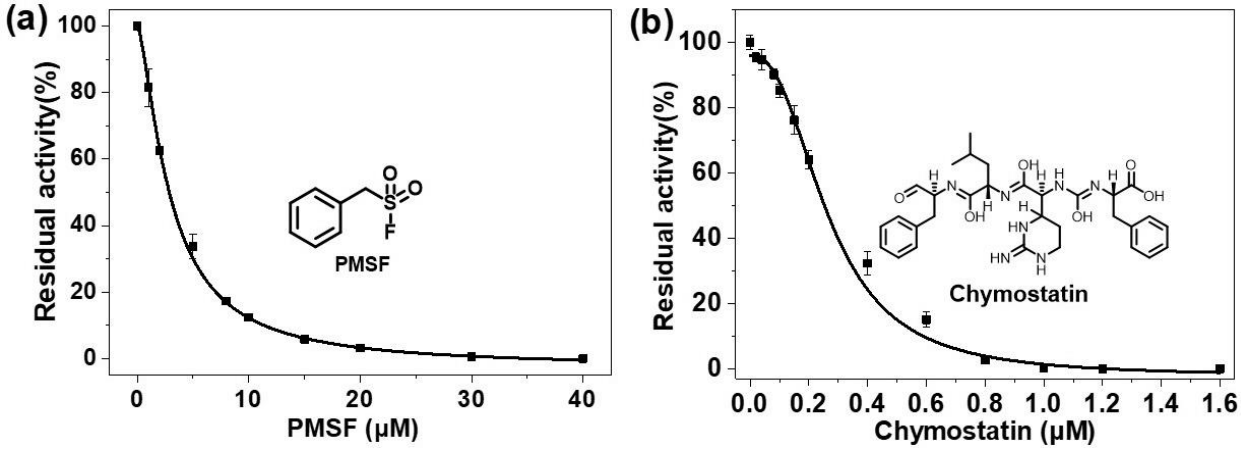

Fig. 7 Plots of inhibitory efficiency of PMSF (a) and chymostatin (b) towards **20** (10 μM) in HEPES buffer (100 mM, ≤ 0.5% DMSO, pH = 8.0) at 30 ºC.

Live Imaging in *Zebrafish*

To further evaluate the possibility of detecting the endogenous chymotrypsin in living systems, we exposed the *zebrafishes* to the probe **20** with and without the addition of the commonly used protease inhibitor *N-tosyl-L-phenylalanyl chloromethyl ketone* (TPCK). Basically, the *zebrafishes* were classified into three groups: group a (as the control) treated with only probe **20**; group b treated with the representative cholinesterase inhibitor (tacrine), and group c treated with TPCK before the incubation with probe **20**. Only after incubation for 10 min with probe **20**, confocal fluorescence microscopy images of *zebrafishes* were recorded and group a showed a strong green fluorescence in the abdomen of *zebrafishes* (Fig. 8a). On the contrary, green fluorescence of the *zebrafishes* pre-treated with TPCK was almost eliminated, whereas no significant change of the green fluorescence was observed for the *zebrafishes* pre-treated with tacrine (Fig. 8b and Fig. 8c). These experimental results showed that probe is an ideal tool for imaging and tracking chymotrypsin in living organisms.

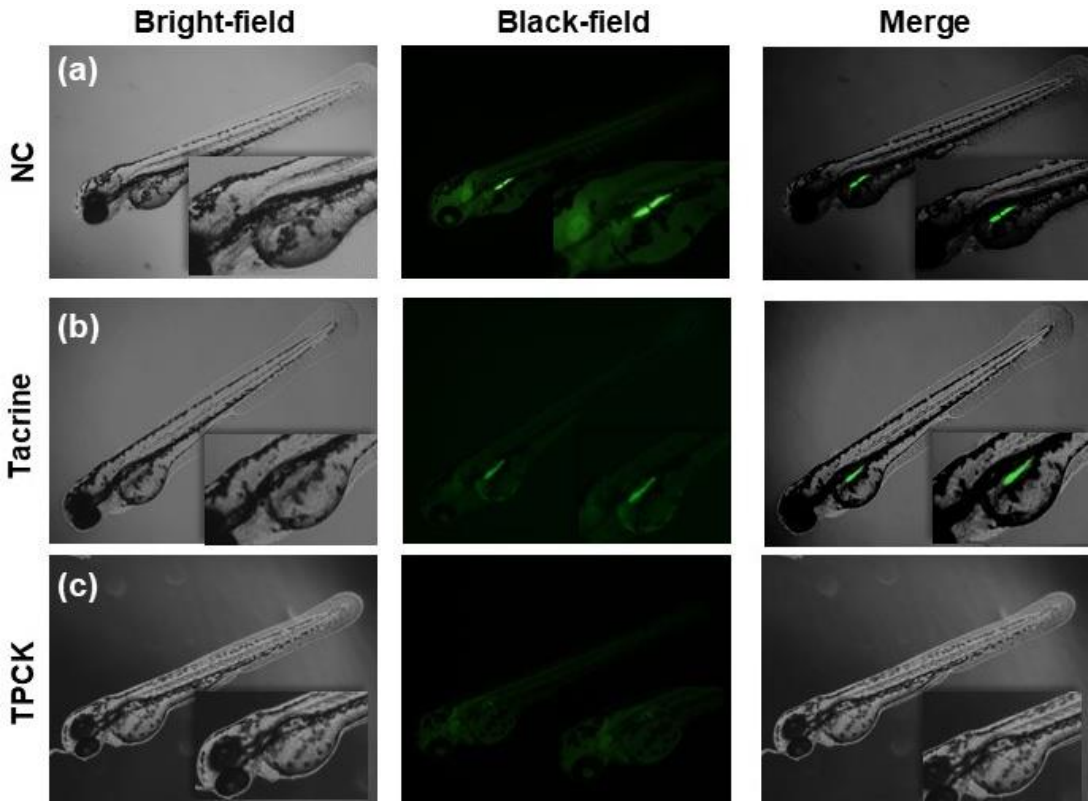

Fig. 8 The *in vivo zebrafish* imaging of probe **20** (5 μM) after incubation without **(**a**)** and with the pre-incubation of 2 μM tacrine **(**b) and 2 μM TPCK (c) for 10 min at room temperature. The panels in each group from left to right represent grayscale of the bright fields, dark fields and the merges of the bright fields and dark fields. The inset in each photo shows a close-up view.

CONCLUSIONS

In summary, we have presented a novel design strategy of MDVS for the generation of fluorescence-quenched substrates for chymotrypsin. The identified probe (**20**) is very efficiently quenched when intact but causes an increased fluorescence of about 250-fold when hydrolytically cleaved by chymotrypsin. In addition, chymotrypsin showed about 16-fold higher binding affinity against probe **20** than the most widely used peptide substrate (**AMC-FPAA-Suc**). The kinetic characterization of its inhibitors with the probe **20**-based fluorometric assay also

proved that it is an efficient tool for chymotrypsin-targeted drug discovery. Most importantly, probe **20** successfully imaged endogenous chymotrypsin in *zebrafishes*. To the best of our knowledge, this is the first reported *in vivo* chymotrypsin imaging with nonpeptide-based fluorescent probe, demonstrating that probe is an effective biosensor in the detection of exogenous and endogenous chymotrypsin in complicated biological samples. With regard to longer-term impacts, the MDVS strategy of identifying fluorescence-quenched substrates may provide general application in the investigation of other enzymes.

ASSOCIATED CONTENT

Supporting Information

Probe library for chymotrypsin, ^{1}H NMR/ ^{13}C NMR spectra for the synthesized probes and Figures for the characterization of the probes (Absorption/ Fluorescence spectra and Inhibitor study with **AMC-FPAA-Suc**).

Acknowledgment

We are grateful for the financial support from the National Key Research and Development Program of China (No. 2017YFA0505200) and the National Natural Science Foundation of China (No. 21332004 and 21672079); Hubei Province Natural Science Foundation (No. 2018CFA072); the self-determined research funds of Central China Normal University (CCNU18ZDPY01 and CCNU18TS007) from the colleges' basic research and operation of MOE".

REFERENCES

1. Farhadian, S.; Shareghi, B.; Saboury, A. A.; Momeni, L., Counteraction of Lactose on the Thermal Stability and Activity of Alpha-Chymotrypsin: Thermodynamic, Kinetic and Docking Studies. *RSC Adv.* **2016,** *6*, 72201-72212.
2. Shah, D.; Mital, K., The Role of Trypsin:Chymotrypsin in Tissue Repair. *Adv. Ther.* **2018,** *35*, 31-42.
3. Domazou, A. S.; Zhu, H.; Koppenol, W. H., Fast Repair of Protein Radicals by Urate. *Free Radical Biol. Med.* **2012,** *52*, 1929-1936.
4. Hoffmann, D. C.; Textoris, C.; Oehme, F.; Klaassen, T.; Goppelt, A.; Romer, A.; Fugmann, B.; Davidson, J. M.; Werner, S.; Krieg, T.; Eming, S. A., Pivotal Role for Alpha1-Antichymotrypsin in Skin Repair. *J. Biol. Chem.* **2011,** *286*, 28889-28901.
5. Yamashita, S.; Sakabe, M.; Ishizawa, T.; Hasegawa, K.; Urano, Y.; Kokudo, N., Visualization of the Leakage of Pancreatic Juice Using a Chymotrypsin-Activated Fluorescent Probe. *Br. J. Surg.* **2013,** *100*, 1220-1228.
6. Moffitt, K. L.; Walker, B.; Martin, S. L., Chymotrypsin-Like Serine Proteinases are Involved in the Maintenance of Cell Viability. *Biochimie* **2012,** *94*, 2582-2589.
7. Zhou, J.; Sahin-Toth, M., Chymotrypsin C Mutations in Chronic Pancreatitis. *J. Gastroenterol. Hepatol.* **2011,** *26*, 1238-1246.
8. Oldziej, A.; Bolkun, L.; Galar, M.; Kalita, J.; Ostrowska, H.; Romaniuk, W.; Kloczko, J., Assessment of Proteasome Concentration and Chymotrypsin-Like Activity in Plasma of Patients with Newly Diagnosed Multiple Myeloma. *Leuk. Res.* **2014,** *38*, 925-930.
9. Beer, S.; Sahin-Toth, M., Clinical Relevance of Chymotrypsin C (CTRC) Mutations in Chronic Pancreatitis. *Pancreas* **2011,** *40*, 1313-1314.
10. Schnermann, M. J., Chemical Biology: Organic Dyes for Deep Bioimaging. *Nature* **2017,** *551*, 176-177.
11. Xiong, L.; Ma, J.; Huang, Y.; Wang, Z.; Lu, Z., Highly Sensitive Squaraine-Based Water-Soluble Far-Red/Near-Infrared Chromofluorogenic Thiophenol Probe. *ACS Sens.* **2017,** *2*, 599-605.
12. Wei, P.; Yuan, W.; Xue, F.; Zhou, W.; Li, R.; Zhang, D.; Yi, T., Deformylation Reaction-Based Probe for In Vivo Imaging of HOCl. *Chem. Sci.* **2018,** *9*, 495-501.

13. Wang, F.; Xu, G.; Gu, X.; Wang, Z.; Wang, Z.; Shi, B.; Lu, C.; Gong, X.; Zhao, C., Realizing Highly Chemoselective Detection of H2S in Vitro and in Vivo with Fluorescent Probes inside Core-Shell Silica Nanoparticles. *Biomaterials* **2018,** *159*, 82-90.

14. Ponnuvel, K.; Ramamoorthy, J.; Sivaraman, G.; Padmini, V., Merocyanine Dye-Based Fluorescent Chemosensor for Highly Selective and Sensitive Detection of Hypochlorous Acid and Imaging in Live Cells. *ChemistrySelect* **2018,** *3*, 12150-12154.

15. Kumar, V.; Rana, H.; Raviraju, G.; Gupta, A. K., Chemodosimeter for Selective and Sensitive Chromogenic and Fluorogenic Detection of Mustard Gas for Real Time Analysis. *Anal. Chem.* **2018**, 1417-1422.

16. Zhang, L.; Duan, D.; Liu, Y.; Ge, C.; Cui, X.; Sun, J.; Fang, J., Highly Selective Off-On Fluorescent Probe for Imaging Thioredoxin Reductase in Living Cells. *J. Am. Chem. Soc.* **2014,** *136*, 226-233.

17. Tan, Y.; Zhang, L.; Man, K. H.; Peltier, R.; Chen, G.; Zhang, H.; Zhou, L.; Wang, F.; Ho, D.; Yao, S. Q.; Hu, Y.; Sun, H., Reaction-Based Off-On Near-infrared Fluorescent Probe for Imaging Alkaline Phosphatase Activity in Living Cells and Mice. *ACS Appl. Mater. Interfaces* **2017,** *9*, 6796-6803.

18. Zhao, X. R.; Chen, Y. L.; Wang, L.; Wang, W. F.; Chen, X. G., Highly Sensitive Fluorescence Detection of Trypsin Based on Gold Nanoparticle Probes. *Anal. Methods* **2016,** *8*, 393-400.

19. Pan, S.; Jang, S. Y.; Liew, S. S.; Fu, J.; Wang, D.; Lee, J. S.; Yao, S. Q., A Vinyl Sulfone-Based Fluorogenic Probe Capable of Selective Labeling of PHGDH in Live Mammalian Cells. *Angew. Chem., Int. Ed.* **2018,** *57*, 579-583.

20. Shen, S.-L.; Zhang, X. F.; Ge, Y.-Q.; Zhu, Y.; Lang, X. Q.; Cao, X. Q., A Near-Infrared Lysosomal pH Probe Based on Rhodamine Derivative. *Sens. Actuators, B* **2018,** *256*, 261-267.

21. Chen, J.; Li, D.; Chi, W.; Liu, G.; Liu, S. H.; Liu, X.; Zhang, C.; Yin, J., A Highly Reversible Mechanochromic Difluorobenzothiadiazole Dye with Near-Infrared Emission. *Chemistry* **2018,** *24*, 3671-3676.

22. Hartmann, A.; Berndt, F.; Ollmann, S.; Krainer, G.; Schlierf, M., In Situ Temperature Monitoring in Single-Molecule FRET Experiments. *J. Chem. Phys.* **2018,** *148*, 123330-123330.

23. Xiong, H.; Yang, J. Q.; Kang, W. M.; Wu, F. X.; Zuo, J. L.; Zhou, Z. Y.; Yang, W. C.; Yang, G. F., Fluorogenic and Chromogenic Detection of Carboxypeptidase Y with a Nonpeptide-Based Small-Molecule Probe. *Sens. Actuators, B* **2018,** *269*, 127-134.

24. Yang, S. H.; Sun, Q.; Xiong, H.; Liu, S. Y.; Moosavi, B.; Yang, W. C.; Yang, G. F., Discovery of a Butyrylcholinesterase-Specific Probe via a Structure-Based Design Strategy. *Chem. Commun. (Cambridge, U. K.)* **2017,** *53*, 3952-3955.

25. Wu, L.; Yang, S. H.; Xiong, H.; Yang, J. Q.; Guo, J.; Yang, W. C.; Yang, G. F., Nonpeptide-Based Small-Molecule Probe for Fluorogenic and Chromogenic Detection of Chymotrypsin. *Anal. Chem.* **2017,** *89*, 3687-3693.

26. Sun, Q.; Li, J.; Liu, W.-N.; Dong, Q. J.; Yang, W. C.; Yang, G. F., Non-Peptide-Based Fluorogenic Small-Molecule Probe for Elastase. *Anal. Chem.* **2013,** *85*, 11304-11311.

27. Moulin, A.; Bell, J. H.; Pratt, R. F.; Ringe, D., Inhibition of Chymotrypsin by a Complex of Ortho-Vanadate and Benzohydroxamic Acid: Structure of the Inert Complex and Its Mechanistic Interpretation. *Biochemistry* **2007,** *46*, 5982-5990.

28. Morris, G. M.; Huey, R.; Lindstrom, W.; Sanner, M. F.; Belew, R. K.; Goodsell, D. S.; Olson, A. J., AutoDock4 and AutoDockTools4: Automated docking with selective receptor flexibility. *J. Comput. Chem.* **2009,** *30*, 2785-2791.

29. Berg, J. M.; Tymoczko, J. L.; Stryer, L., *Biochemistry*. 5th ed.; W H Freeman: San Francisco, 2002.

30. Hou, S.; Xue, L.; Yang, W.; Fang, L.; Zheng, F.; Zhan, C. G., Substrate selectivity of high-activity mutants of human butyrylcholinesterase. *Org. Biomol. Chem.* **2013,** *11*, 7477-7485.

31. Fang, L.; Chow, K. M.; Hou, S.; Xue, L.; Chen, X.; Rodgers, D. W.; Zheng, F.; Zhan, C. G., Rational Design, Preparation, and Characterization of a Therapeutic Enzyme Mutant with Improved Stability and Function for Cocaine Detoxification. *ACS Chem. Biol.* **2014,** *9*, 1764-1772.

32. Xu, H.; Hepel, M., "Molecular beacon"-based fluorescent assay for selective detection of glutathione and cysteine. *Anal. Chem.* **2011,** *83*, 813-819.

33. Ogren, P. J.; Meetze, A.; Duer, W. C., The Limit of Detection in Generalized Least-Squares Calibrations: An Example Using Alprazolam Liquid Chromatography-Tandem Mass Spectrometry Data. *J. Anal. Toxicol.* **2009,** *33*, 129-142.

TOC

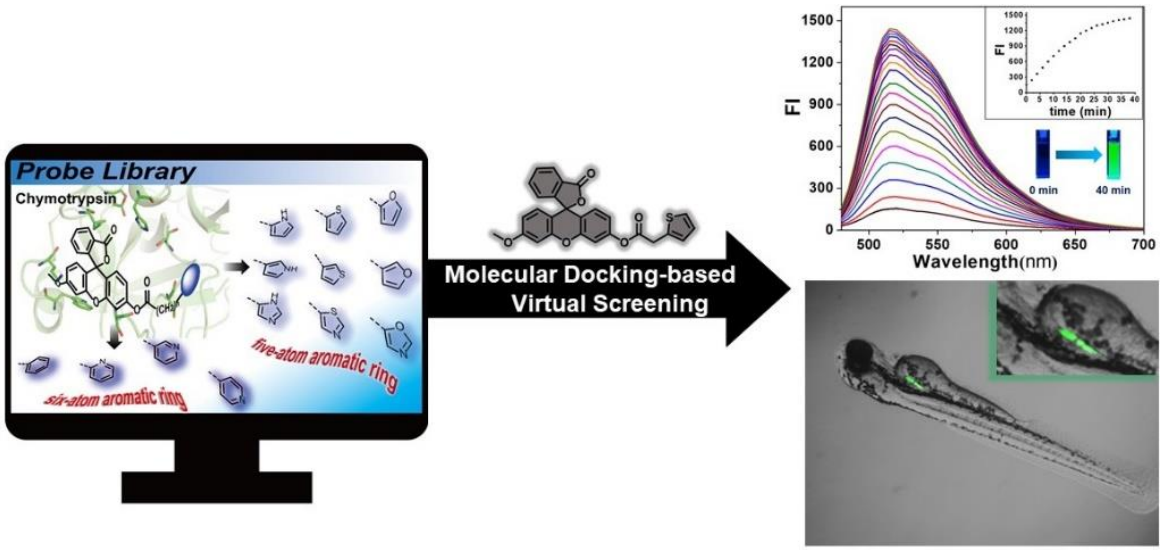
Probe Library
Chymotrypsin
six-atom aromatic ring
five-atom aromatic ring
Molecular Docking-based
Virtual Screening
FI
Wavelength(nm)
time (min)
0 min
40 min